Supporting Information

Degradable Self-Adhesive Epidermal Sensors Prepared from Conductive Nanocomposite Hydrogel

Zhiang Shao, Xiangming Hu, Weimin Cheng*, Yanyun Zhao, Jiaoyun Hou, Mingyue Wu, Di Xue, and Yuhao Wang*

College of Safety and Environmental Engineering, Shandong University of Science and Technology Qingdao, Shandong 266590, China

*Corresponding E-mail:
xiangming0727@163.com
wmcheng@sdust.edu.cn

Scanning Electron Microscope (SEM) of the freeze-dried hydrogel

In order to verify the hydrogel's structure, the hydrogel was first freeze-dried (-80 °C) overnight to remove excess moisture while its original three-dimensional network structure was maintained. Then, the freeze-dried specimens were broken apart, and the inner morphology of the various hydrogels was observed by SEM (JSM 6390, JEOL, Japan). It can be seen from Figure S3a and c that the conductive hydrogels has more smaller pore size and thicker pore wall structure than PAM hydrogel, indicating that the supramolecular interactions between Fe^{3+}, CNF, PDA and PAM is beneficial to promote the association of polymer chains, thereby increasing the mechanical properties of the hydrogel. It can be seen from Figure S3b and d that micro-fibril structure appear in the pores of the conductive hydrogel, but they do not appear in the pure PAM hydrogel. The microfibrils are nanostructures formed by the supramolecular interaction between the polymer chains PAM-PDA-CNF and Fe^{3+}, which are beneficial to increase the conductivity of the hydrogel.

Detailed FTIR characterization of the conductive hydrogels

In order to verify the hydrogen bonding among PAM, CNF and PDA, and metal coordination between PDA/CNF and Fe^{3+}, FTIR spectra of PAM, PAM-CNF, PAM-CNF-Fe^{3+}, and PAM-PDA, PAM-PDA-CNF, and PAM-CNF-PDA-Fe^{3+} gels were characterized using FTIR spectroscopy analyzer. As shown in Figure S5, PAM displayed characteristic peaks at 3183, 2954, 2855, 1634, 1174, and 1123 cm^{-1}, which can be attributed to the stretching vibration of N-H bond of secondary amine, the anti-symmetric and symmetric stretching vibrations of C-H bond of methylene group, the stretching vibration of C=O bond of amide group, and the anti-symmetric and symmetric stretching vibrations of C-N bond of amide group, respectively. After CNF was introduced, there was a clear red-shift for the antisymmetric stretching vibration peak of C-N bond (1173.25 cm^{-1}) of PAM-CNF, indicating that there was a strong hydrogen bonding between CNF and PAM. PAM-CNF had a wider peak of -OH in -COOH at

3420.87 cm^{-1} and a stretching vibration peak of C=O at 1667.09 cm^{-1} respectively. After Fe^{3+} was added, the hydroxyl peak of PAM-CNF-Fe^{3+} (3419.23 cm^{-1}) red-shifted and clearly became stronger. The peak of C=O of PAM-CNF-Fe^{3+} (1664.82 cm^{-1}) also underwent a red shift, indicating that the carboxyl group changed from the original association state to the chelation state with Fe^{3+}. PAM-PDA showed a wide phenolic hydroxyl peak at the 3422.88 cm^{-1} and a stretching vibration peak of phenolic carbonyl group at 1666.46 cm^{-1}. After the addition of CNF, the carbonyl peak of PAM-CNF-PDA (1655.41cm^{-1}) showed a red shift, indicating that there was strong hydrogen bonding between PDA and CNF. After addition of Fe^{3+}, the hydroxyl peak intensity of PAM-CNF-PDA-Fe^{3+} was higher than that of PAM-PDA and exhibited a significantly red shift, indicating that the original catechol group converted from π - π conjugation to chelate with Fe^{3+}. Compared with that of PAM-CNF-PDA, the carbonyl peak of PAM-CNF-PDA-Fe^{3+} was slightly intensified, probably, because the oxidation of DA by Fe^{3+} increased the carbonyl content of the system.

Rheological characterization of the conductive hydrogels

Figure S7 (a-c) show the variations in storage modulus G' and loss modulus G" of the conductive hydrogels over the angular frequency ranging from 0.01 to 100 rad s^{-1}. The tested conductive hydrogel samples had different DA contents (1‰, 2‰, and 4‰ wt/AM), different Fe^{3+} contents (c_{Fe3+}:c_{DA} = 0.5, 1, and 2) and different CNF contents (0.25%, 0.375%, and 0.5% wt/water) and were tested under a constant strain (λ = 1.0%, linear interval). For determining the linear viscoelastic region, the conductive hydrogels was first subjected to scan test with varying strain amplitudes (0.01~100%).[1] As shown in Figure S6a, as the DA content increased from 1‰ to 2‰, the storage modulus of the conductive hydrogels increased significantly, indicating that the proper amount of DA can enhance the content of crosslinked structure in the conductive hydrogels. As the content of DA further increased to 4‰, the the conductive hydrogels's storage modulus decreased as DA can weaken the activity of APS and

then block the free radical polymerization in the gel system.[2] Therefore, when the DA content was 2‰, the conductive hydrogels could obtain better enhancing effect. Fe^{3+} also exhibited similar situation with DA. As shown in Figure S6b, as the molar ratio of Fe^{3+} to DA increased from 0.5 to 1, the storage modulus of the conductive hydrogels increased significantly, indicating that in addition to chelating with DA, the remaining Fe^{3+} could continue to chelate with CNF, thereby, enhancing the strength of gel (it is generally considered that a stable tris-catechol-Fe^{3+} complexes can easily form when the molar ratio between Fe^{3+} and DA is about 1:3). [3] As the molar ratio of Fe^{3+} to DA increased to 2, the storage modulus of the conductive hydrogels contrarily decreased, primarily, because the excessive Fe^{3+} may have over-oxidized DA; thereby, reducing the content of catechol group in the conductive hydrogels, and then, weakening the crosslinking structure in the conductive hydrogels. As shown in Figure S7c, the storage modulus increased as the CNF content in the system increased. Compared with the case containing higher CNF concentration (0.5 wt%), when the CNF contents were 0.25% and 0.375%, the storage modulus became extremely low, and the loss modulus and storage modulus became very close. The variation in moduli indicates that the conductive hydrogels had low crosslink density and a tendency of converting to sol, which indirectly indicates that CNF are the main physically-crosslinked sites of the conductive hydrogels.

Gel permeation chromatography (GPC) characterization of gel solution

In the section, two PS Mix (250×7 mm, dp = 5 μm) and two PS-1 (250 × 7 mm, dp = 5 μm) columns were adopted. Water was used as the mobile phase, RID 7490 as refractive index detector, and UV diode-array detector were used in series. All the samples were separated at 20°C. The flowrate of mobile phase was 2 ml/min and the injected volume of sample was 100 μL. Before entering columns, the solution was filtered through a 0.45 μm PTFE membrane. For determining the molecular weight, a calibration curve was drawn by using standard

polyacylamide samples with known molecular weights (218,000, 85,600, 40,000, 20,000, 8,000, 6,000, 4,000, and 1,000 Da). In order to accurately reflect the molecular weight change of polymer in the solution with time, a standard curve was drawn by measuring the gel solution (50 mg/ml) after degradation at different times (0 day, 7 days, 14 days, and 30 days). Various molecular-weight parameters of the gel solution are listed in Table S4. A GPC molecular-weight distribution calibration curve [$\log M = f(V_e)$] was drawn based on the data in Table S5 (Figure S10). The eight points on the calibration curve represent polyacrylamide with molecular weights of 218000, 85600, 40,000, 20,000, 8000, 6000, 4000, and 1000 Da and water (18 Da), respectively.

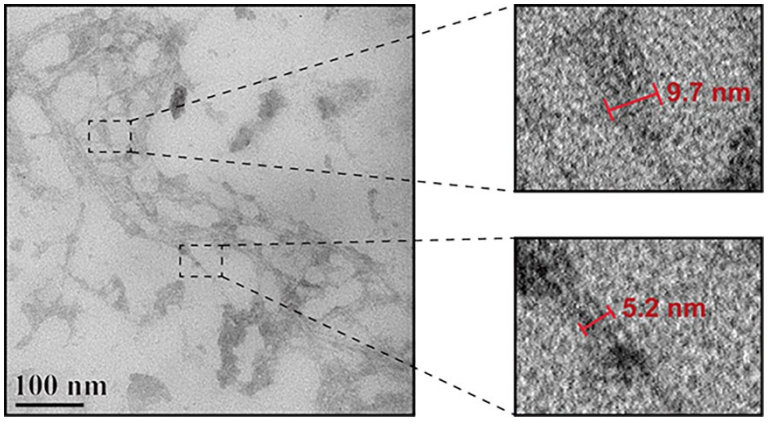

Figure S1. TEM images of CNF.

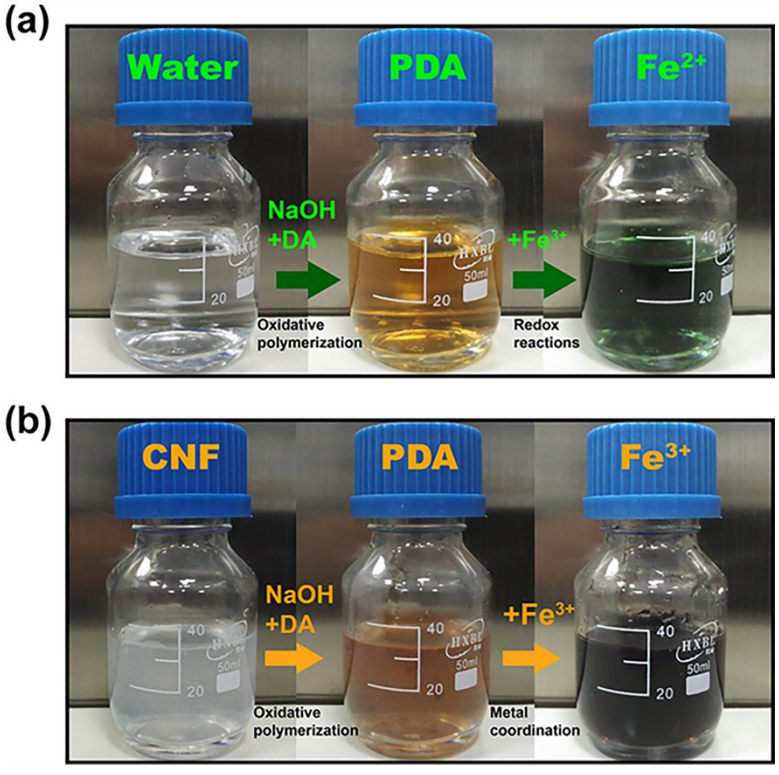

Figure S2. The color variation when Fe^{3+} co-existed with DA (a) in water and (b) in CNF solution.

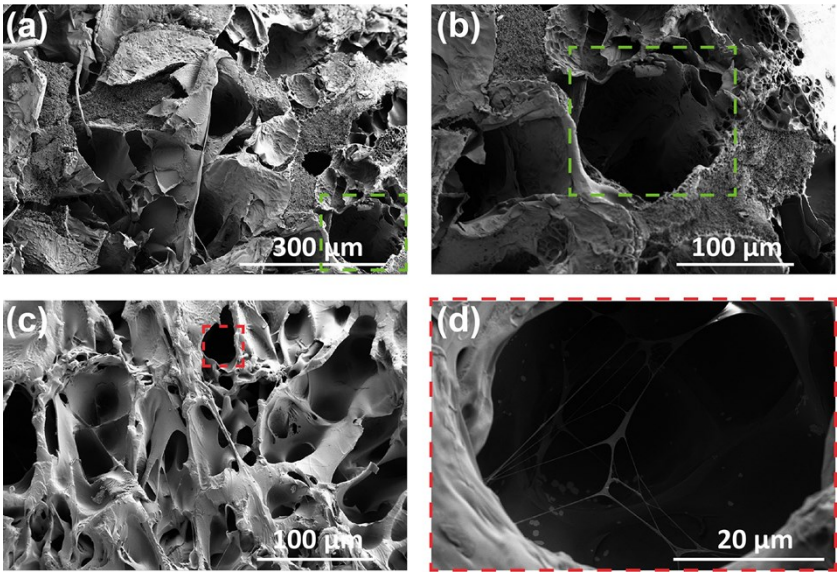

Figure S3. SEM images of (a-b) the PAM hydrogel, (c) the conductive hydrogels, and (d) microfibrils embedded in the the conductive hydrogels.

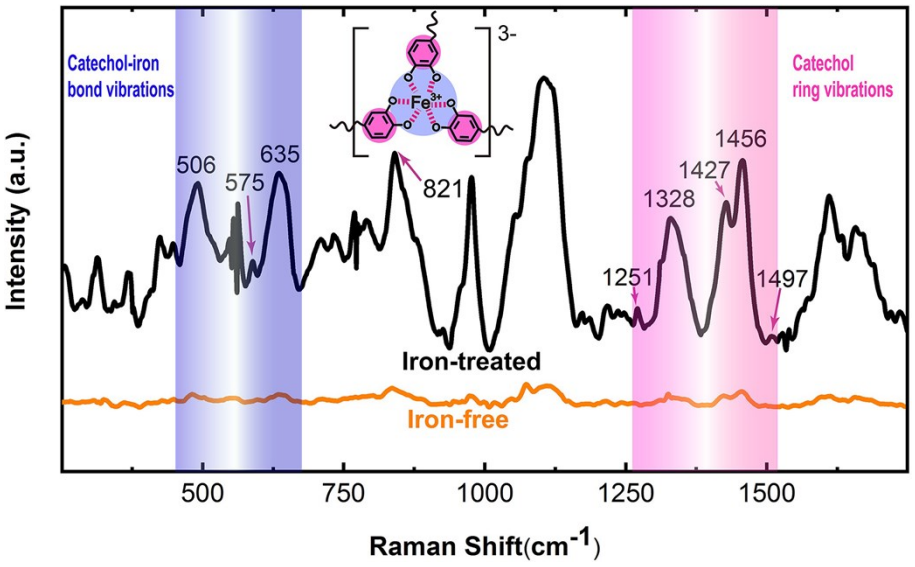

Figure S4. Raman spectra of the conductive hydrogels with Fe^{3+} (black curve) and without Fe^{3+} (orange curve).

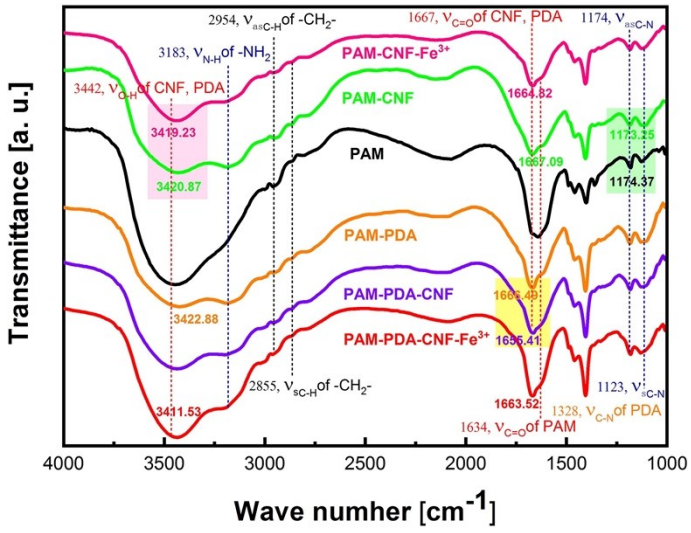

Figure S5. FTIR spectra of the freeze-dried conductive hydrogels with different components.

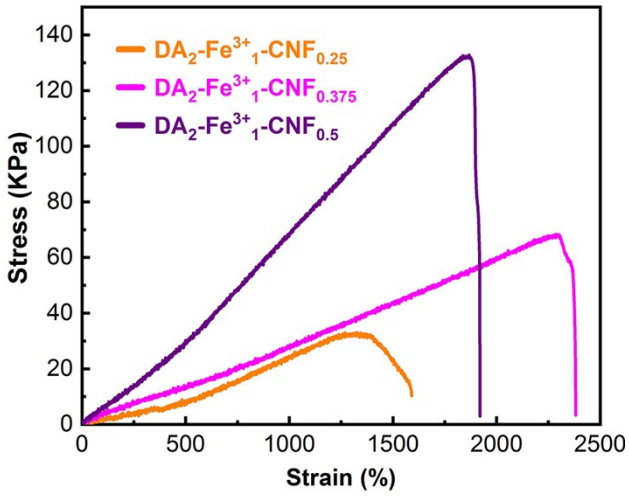

Figure S6. Tensile stress-strain curves of the conductive hydrogels with different content of CNF.

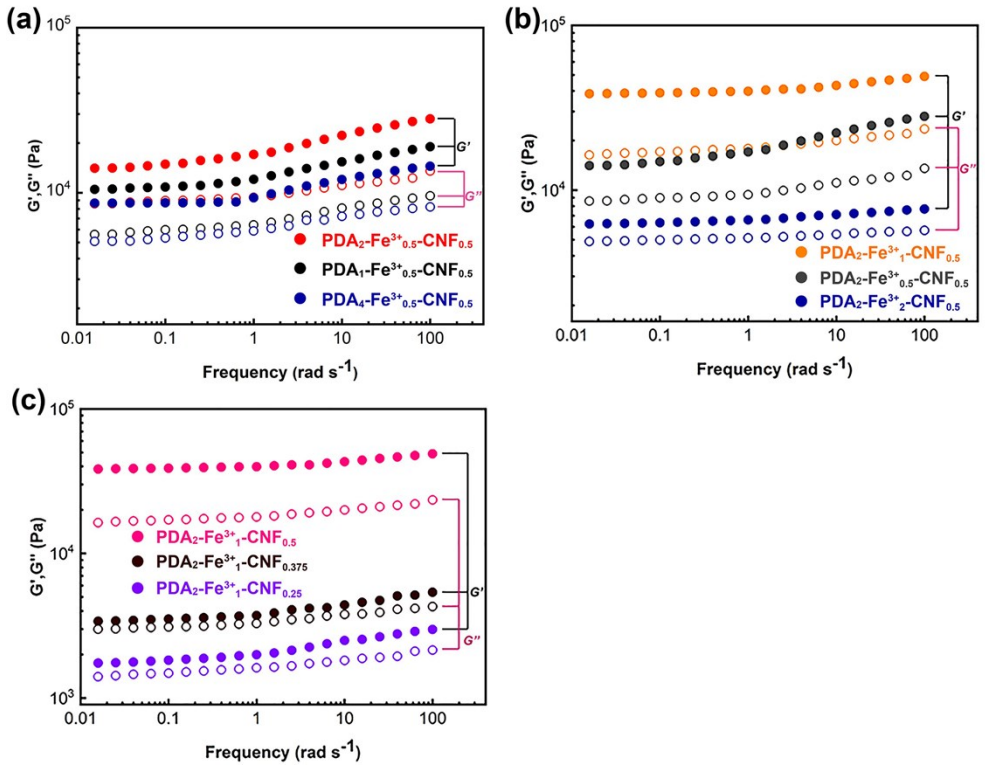

Figure S7. Storage modulus G' and loss modulus G" of the conductive hydrogels with different DA contents (a), c_{Fe3+}:c_{DA} (b) and CNF contents (c).

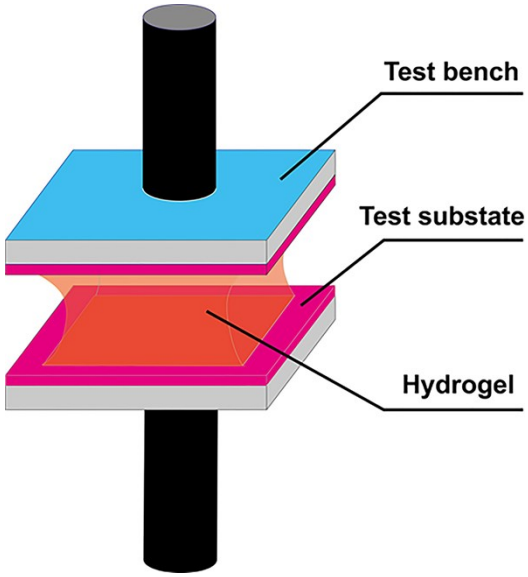

Figure S8. Diagram of device to measure the self-adhesive performance.

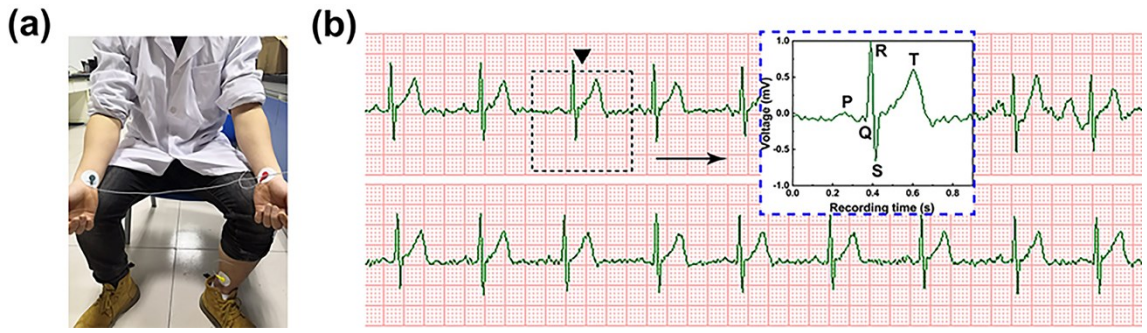

Figure S9. (a) Ag-AgCl commercial electrode adhered to arteries of human limbs; (b) Ag-AgCl commercial electrode to measure the ECG of human body.

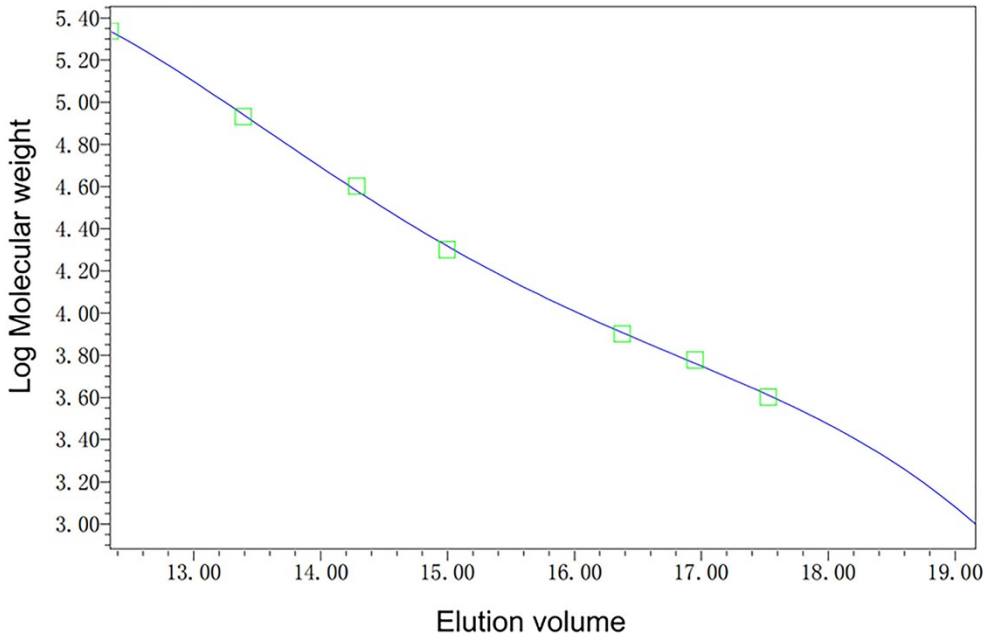

Figure S10. GPC calibration curve of the conductive hydrogels polymer solutions.

Table S1. Composition of the conductive hydrogels with different DA contents.

code	CNF/water (wt%)	CNF solution (ml)	DA (mg)	$FeCl_3$ (mg)	AM (g)	APS (g)	TEMED (μl)	MBA（mg）
DA_0-$Fe^{3+}_{0.5}$-$CNF_{0.5}$	0.5	20	0	4	5.5	0.6	40	10
DA_1-$Fe^{3+}_{0.5}$-$CNF_{0.5}$	0.5	20	6	4	5.5	0.6	40	0
DA_2-$Fe^{3+}_{0.5}$-$CNF_{0.5}$	0.5	20	12	8	5.5	0.6	40	0
DA_4-$Fe^{3+}_{0.5}$-$CNF_{0.5}$	0.5	20	24	16	5.5	0.6	40	0

According to different amounts of DA, Fe^{3+} and CNF, the prepared conductive hydrogels were termed as DA_x-Fe^{3+}_y-CNF_z, where x, y, and z refer to the mass percentage of DA to AM (x), the molar concentration ratio between Fe^{3+} and DA, and the mass percentage of CNF to water (z%).

Table S2. Composition of the conductive hydrogels with different Fe^{3+} contents.

code	CNF/water (wt%)	CNF solution (ml)	DA (mg)	$FeCl_3$ (mg)	AM (g)	APS (g)	TEMED (μl)
DA_2-$Fe^{3+}_{0.5}$-$CNF_{0.5}$	0.5	20	12	8	5.5	0.6	40
DA_2-Fe^{3+}_{1}-$CNF_{0.5}$	0.5	20	12	16	5.5	0.6	40
DA_2-$Fe^{3+}_{1.5}$-$CNF_{0.5}$	0.5	20	12	24	5.5	0.6	40
DA_2-Fe^{3+}_{2}-$CNF_{0.5}$	0.5	20	12	32	5.5	0.6	40

Table S3. Composition of the conductive hydrogels with different CNF contents.

code	CNF/water (wt%)	CNF solution (ml)	DA (mg)	$FeCl_3$ (mg)	AM (g)	APS (g)	TEMED (μl)	MBA（mg）
DA_2-Fe^{3+}_1-CNF_0	0	20	12	16	5.5	0.6	40	10
DA_2-Fe^{3+}_1-$CNF_{0.25}$	0.25	20	12	16	5.5	0.6	40	0
DA_2-Fe^{3+}_1-$CNF_{0.375}$	0.375	20	12	16	5.5	0.6	40	0
DA_2-Fe^{3+}_1-$CNF_{0.5}$	0.5	20	12	16	5.5	0.6	40	0

Table S4. GPC measuring index and results of gel solutions.

	Mn (Da)	Mw (Da)	MP (Da)	Mz (Da)	Mz+1 (Da)	Poiydispersity
Original	73300	117853	211200	147381	163973	1.607814
7 day	36252	83021	154921	127688	153113	2.290110
14 day	24759	62125	100207	108938	140300	2.509215
30 day	1335	1361	1338	1338	1416	1.019698

Table S5. Calibration curves of gel solutions.

	Molecular weight (Da)	Retention time (min)	Calculated weight (Da)	Residual (%)
1	218000	12.358	217271	0.335
2	40000	14.288	38025	5.194
3	8000	16.397	8099	-1.219
4	4000	17.554	4092	-2.256
5	85600	13.391	87488	-2.158
6	20000	15.007	20793	-3.814
7	6000	16.982	5761	4.145
8	1000	19.179	999	0.118

Reference:

[1] Q. G. Wang, J. L. Mynar, M. Yoshida, E. Lee, M. Lee, K. Okuro, K. Kinbara, T. Aida, *Nature*, **2010**,*463* , 339.

[2] L. Han, L. W. Yan, K. F. Wang, L. M. Fang, H. P. Zhang, Y. H. Tang, Y. H. Ding, L. T. Weng, J. L. Xu, J. Weng, Y. J. Liu, F. Z. Ren, X. Lu, *NPG Asia Mater* 9, e372 (**2017**) doi:10.1038/am.2017.33.

[3] S. Hou, P. X. Ma, *Chem Mater.* **2015**, *27*, 7627.